Pancreatology xxx (xxxx) xxx

Contents lists available at ScienceDirect

Pancreatology

journal homepage: www.elsevier.com/locate/pan

Altered centriolar cohesion by CEP250 and appendages impact outcome of patients with pancreatic cancer

Guido Giordano [a, **], Giampiero Cipolletta [b], Agostino Mellone [b], Giovanni Puopolo [b], Luigi Coppola [c], Elena De Santis [d], Nicola Forte [e], Francesco Napolitano [b], Francesca P. Caruso [f, g], Paola Parente [h], Matteo Landriscina [a], Luigi Cerulo [b, g], Maria Claudia Costa [f, g, ***], Massimo Pancione [b, i, *]

[a] Unit of Medical Oncology and Biomolecular Therapy, Department of Medical and Surgical Sciences, University of Foggia, Policlinico Riuniti, 71122, Foggia, Italy
[b] Department of Science and Technology, University of Sannio, Benevento, Italy
[c] UOC Anatomia ed Istologia Patologica e Citologia Diagnostica, Dipartimento dei Servizi Diagnostici e della Farmaceutica, Ospedale Sandro Pertini, ASL Roma 2, 00157, Rome, Italy
[d] Department of Anatomical Histological Forensic Medicine and Orthopedic Sciences, Sapienza University of Rome, 00185, Roma, Italy
[e] Department of Clinical Pathology, Fatebenefratelli Hospital, 82100, Benevento, Italy
[f] Department of Electrical Engineering and Information Technology, University of Naples - Federico II, Italy
[g] Bioinformatics Laboratory, BIOGEM scrl, Ariano Irpino, Avellino, Italy
[h] Unit of Pathology, Fondazione IRCCS, Hospital House for the Relief of Suffering, San Giovanni Rotondo, Foggia, Italy
[i] Department of Biochemistry and Molecular Biology, Faculty of Pharmacy, Complutense University Madrid, 28040, Madrid, Spain

ARTICLE INFO

Article history:
Received 20 February 2024
Received in revised form
2 June 2024
Accepted 24 June 2024

Keywords:
Pancreatic ductal adenocarcinoma
Centrosome linker. centriolar appendages
CEP250
CEP170
CEP164

ABSTRACT

Background: Pancreatic ductal adenocarcinoma (PDAC) is one of the leading cause of cancer death worldwide. PDACs are characterized by centrosome aberrations, but whether centrosome-related genes influence patient outcomes has not been tested.
Methods: Publicly available RNA-sequencing data of patients diagnosed with PDAC were interrogated with unsupervised approaches to identify centrosome protein-encoding genes with prognostic relevance. Candidate genes were validated by immunohistochemistry and multiplex immunofluorescence in a set of clinical PDAC and normal pancreatic tissues.
Results: Results showed that two genes *CEP250* and *CEP170*, involved in centrosome linker and centriolar subdistal appendages, were expressed at high levels in PDAC tissues and were correlated with prognosis of PDAC patients in independent databases.
Large clustered γ-tubulin-labelled centrosomes were linked together by aberrant circular and planar-shaped CEP250 arrangements in CEP250-high expressing PDACs. Furthermore, PDACs displayed prominent centrosome separation and reduced CEP164-centrosomal labelling associated with acetylated-tubulin staining compared to normal pancreatic tissues. Interestingly, in a small validation cohort, CEP250-high expressing patients had shorter disease free- and overall-survival and almost none of those who received gemcitabine plus nab-paclitaxel first-line therapy achieved a clinical response. In contrast, weak CEP250 expression was associated with long-term survivors or responses to medical treatments.
Conclusions: Alteration of the centriolar cohesion and appendages has effect on the survival of patients with PDAC.

* Corresponding author. Department of Science and Technology, University of Sannio, Benevento, Italy.
** Corresponding author.
*** Corresponding author. Department of Electrical Engineering and Information Technology, University of Naples - Federico II, Italy.
E-mail addresses: guido.giordano@unifg.it (G. Giordano), mariaclaudiacosta00@gmail.com (M.C. Costa), massimo.pancione@unisannio.it (M. Pancione).

https://doi.org/10.1016/j.pan.2024.06.010
1424-3903/

1. Introduction

Pancreatic Cancer (PDAC) is a lethal disease, accounting as the fourth cause of cancer-related deaths in Western Countries [1]. Late diagnosis, subtle clinical presentation, resistance to current treatments and biological complexity, represent the major issues underlying its terrible prognosis [2]. Nowadays, radical surgery, when feasible, remains the only chance to potentially cure patients. Systemic therapy, indeed, is the unique weapon to face advanced disease [3–5]. In contrast with other cancers, molecular subtyping of pancreatic cancer is not clearly defined and remains without clinically relevant morphological or molecular classification. Early molecular profiling studies suggested a putative pathological progression model, analogous to the adenoma-carcinoma model in the colon [6,7]. Previous studies demonstrated that the combined expression of oncogenic Kras, coupled with the deletion or loss of function of Tp53, Cdkn2a readily leads to invasive PDAC [7,8]. Recent advances in nucleic acid sequencing paved the way to identify previously unrecognized genomic, epigenomic and transcriptomic subtypes of human PDAC [9–11]. For example, Bailey and colleagues identified four subtypes of PDAC, which they termed “Squamous”, “Pancreatic Progenitor”, “Immunogenic” and “Aberrantly Differentiated Endocrine Exocrine (ADEX)” [11]. So far, the Squamous, Quasi-mesenchymal and Basal-like subtypes discovered in the above mentioned studies are fairly well aligned across all three classification systems and appear to be associated with a poor prognosis [9–11]. Despite the mentioned significant progress, unfortunately, these have not translated into a breakthrough in clinical care for the majority of patients.

Recently, numerical and structural centrosome dysfunction has gained attention for its potential relevance in cancer [12]. However, it is unknown whether centrosome anomalies contribute to the disease and patient outcomes.

The centrosome is a tiny membrane-less condensate composed of centrioles surrounded by pericentriolar material (PCM) [13]. It is well known as the main microtubule-organizing center (MTOC) of the animal cells and as organizer of cilia, membrane-bound antenna-like extensions [14]. When a cell initiates division, the PCM grows and increases microtubule nucleation, while centriole proximal end cohesion factors such as C-Nap1, (also known as CEP250) and rootletin (also known as CROCC), are disassembled to separate sister centrosomes [13]. The two centrioles in the centrosome differ in age, functional activity and the presence of additional structures associated with their surface [15]. The centriole possessing the distal (DAPs) and subdistal (sDAPs) appendages is older and referred to as the mother centriole, whereas the other centriole lacking appendages is the daughter centriole [15]. DAPs proteins are indispensable for the early steps of primary ciliogenesis, the disruption of which is associated with a broad range of diseases including cancer [16,17]. For example, it has been shown that the suppression of CEP164, one of the major constituents of DAPs, leads to blockage of ciliogenesis [18]. Although interdependent, DAPs and sDAPs appear to be functionally and structurally different [15–18]. Notably, sDAPs proteins including Ninein and CEP170, are located at both the distal and proximal ends of centriole through the centrosome linker factor CEP250 [19,20]. The interdependence of sDAPs and CEP250 is indispensable for the microtubule anchoring proprieties of the cells and the spatial control of the ciliogenesis [21,22]. While it is generally accepted that centrosome dysfunction can result in aberrant cell proliferation, whether these different centrosome substructures affect cancer progression remains unknown. Nevertheless, direct investigations on the PDAC prognosis are not yet available.

We here developed a model to discover and validate potential centrosomal-related genes predictive of PDAC prognosis. We found that centrosome linker and centriolar appendages protein coding genes are inversely deregulated in PDAC tissues.

2. Materials and methods

2.1. Gene expression data

Protein-encoding genes annotated with the location “centrosome and centriolar satellites” (n = 564) were downloaded from the Human Protein Atlas (HPA) [23] and were hereafter referred to as centrosome-related genes (CRGs). Gene Expression data and available clinical information for 96 individuals diagnosed with PDAC were obtained from a gene expression Omnibus dataset (GSE36924) [9]. Of 564 genes, 482 were included in the expression data. PDACs were classified into 4 molecular subtypes according to Bailey et al.: squamous; pancreatic progenitor; immunogenic; and aberrantly differentiated endocrine exocrine (ADEX) [9]. An unsupervised clustering analysis was performed based on the expression of the CRGs. In particular, hierarchical clustering with Ward linkage and Euclidean distance as implemented in the R *hclust* function was used. The optimal number of clusters was chosen based on the Calinski-Harabasz criterion. Gene expression profiles of PDAC and normal pancreatic samples were collected from the Cancer Genome Atlas (TCGA) and Genotype-Tissue Expression (GTEx) databases, respectively [24]. The GEPIA web tool was used to analyze the differential gene expression between PDACs and normal pancreatic tissues [25]. ANOVA (analysis of Variance) with a p-value threshold of 0.05 was performed to detect genes having a significant differential expression among the molecular subtypes. Consensus transcript expression level for a subset of CRGs across all major organs and tissues were based on transcriptomics data from HPA and GTEx [23,24]. The resulting normalized transcript expression levels denoted (nTPM) value was calculated for each gene. Only genes with differential expression in pancreas tissues are shown.

2.2. Constructing a prognostic signature based on CRGs

In order to obtain a predictive model for PDAC patients outcome, we first combined the transcriptomic data and survival information from the PDAC dataset (GSE36924). Moreover, gene expression profiling and survival data from 80 additional PDAC patients (CPTAC) dataset, were used as a test set [26]. To identify CRGs associated with prognosis, univariate Cox regression analysis on the training and test set was performed. The Cox Proportional Hazard (CPH) method was applied using the *coxph*-function from the survival R package. A Wald test FDR $\leq$0.1 was considered as statistically significant. The risk of death associated with the expression of each CRG was modeled through the CPH beta coefficient, interpreted as an increase (for positive values) or a decrease (for negative values). The “forest plot” was used to conduct a multivariate Cox regression analysis for CEP250 expression and clinical features in CPTAC and GSE36924 datasets. Kaplan Meier curves were computed using the Log-Rank test and the *Surv* function from the survival R package. To obtain the survival curve corresponding to each CRG, the first and third quartile of the gene expression distribution was considered in order to define high and low expression, respectively. Over-representation enrichment analysis and gene ontology (GO)-Terms were identified through the DAVID tool (Database for Annotation, Visualization, and Integrated Discovery cite) and g:Profiler [27]. GO-Terms that scored significant in these two tools were included. Unsupervised hierarchical clustering analysis with Complete linkage and Euclidean distance (*hclust* function) has been performed on the expression data of the CRGs prognostic genes. The data were rescaled based on the quartile distributions of the

CRGs expression. The R software package was used to perform differential gene analysis of the HR-group "shared bad prognosis genes" versus the LR-group "shared good prognosis genes". Finally, PDAC patients from the TCGA database were used to analyze the prognostic significance of CEP164.

2.3. Clinical tissue samples

Formalin-fixed paraffin-embedded slides of PDAC (n = 23) and normal pancreatic tissue (n = 4) were procured from three different Institutions, Policlinico Ospedali Riuniti - University of Foggia, Sandro Pertini Hospital of Rome and Casa Sollievo della Sofferenza Hospital, San Giovanni Rotondo, Foggia, Italy. This study was approved by Policlinico Ospedali Riuniti, University of Foggia Ethic Committee (Comitato Etico Area 1, 128/CE/2023). Patients underwent to radical surgical resection between 2017 and 2023 were included in the study. All tumors were histologically diagnosed as PDAC and classified according to the TNM staging system of the International Union Against Cancer (UICC) version 7**.** Clinical and pathological data for each patient were obtained from the medical records and the pathology reports from the archives of the Hospitals involved in the study. The follow-up and death data were collected, and censored at 2023, December 31st. After surgical resection, 19 out of 23 patients received adjuvant therapy with single agent gemcitabine (n = 16) or modified (m)FOLFIRINOX (n = 3) and 17 out of 23 patients relapsed after surgery/adjuvant treatment and received first-line chemotherapy with nab-paclitaxel/gemcitabine combination (Table S1).

2.4. Patients' outcome data

Patients' outcome was evaluated in terms of overall survival (OS) and disease-free survival (DFS). Overall Survival was defined as the time elapsed from the start of adjuvant treatment to death for any cause; DFS was defined as the time from the start of adjuvant treatment and disease progression or death, whichever occurred first. Consistently, in the "relapsed" cohort objective response to first-line chemotherapy and Progression Free Survival (PFS) were evaluated. The best overall response (ORR) was evaluated by Computed Tomography (CT) scan every 8 or 12 weeks following the Referral Oncologists' daily practice. Tumor response was classified in: complete response (CR), partial response (PR), stable disease (SD), and progressive disease (PD) according to Response Evaluation Criteria in Solid Tumors (RECIST). Consequently, patients with CR, PR and SD $\geq$ 6 months were considered responders while the remaining non-responders. Progression Free Survival was defined as the time between the start of first line chemotherapy and disease progression or death, whichever occurred first.

2.5. Immunohistochemistry (IHC) staining

Immunohistochemistry (IHC) was performed with Kit Neostain ABC kit, (NeoBiotech, NB-23-00001-6). Serial sections of normal pancreas and PDAC (4 μm thick) were mounted onto positively charged slides and dried for 24 h. The slides were deparaffinized and rehydrated by washing in xylene three times, 7 min each, followed by passing through 100 %, 75 %, and 50 % ethanol and ddH2O for rehydration. Heat-induced epitope retrieval was performed by heating the slides in 1X NeoUltra Retrieval Solution 20X (NeoBiotech, NB-23-00178-4) for 40 min. The block of endogenous peroxides was done using the 3 % H202 for 4min. Slides were washed in PBS following by blocking buffer (BeoBiotech, NB-26-01605) for 30 min at room temperature. Primary antibodies were incubated at 4 °C for 1 h in a humidified chamber as follows: Anti-C-NAP1 (Proteintech Europe, 66814-1); diluted 1:100; Anti-CEP164 (ABclonal, A9964), diluted 1:250. Slides were then incubated with Biotinylated second antibody (NeoBiotech) for 15 min and HRP (NeoBiotech) for 15 min, respectively. The 3,3′ diaminobenzidine (3 min) and hematoxylin (5 min) were used as chromogen and counterstain, respectively. The antigen-antibody complexes were then revealed with 3,3' diaminobenzidine (DAB) chromogen (3 min) and counterstained with Hematoxylin for 8 min and coverslipped in permanent mounting media (NeoBiotech). The IHC staining pattern was evaluated taking into account the fraction of stained cells as "high >75 %", "moderate 25–75 %" and weak <25 %". Staining at the nucleus, cytoplasm, or membranes was also collected.

2.6. High resolution multiplexed immunofluorescent microscopy

To accurately quantify centrosomes in PDACs and normal pancreatic tissues, we used a multiplex immunofluorescence microscopy–based method as reported [28]. Slides (5-μm) thickness were deparaffined and rehydrated. Antigen retrieval was performed using the Universal HIER antigen retrieval reagent, 10X, diluted 1:10 (ab208572, abcam) and heated at 97 °C using a decloaking chamber for 20 min. Slides were washed in washing buffer (PBS and 0.1 % Tween 20 at 25 °C) following by blocking buffer (BeoBiotech, NB-26-01605) for 30 min at room temperature. Primary antibodies were diluted in blocking buffer and incubated at 4 °C overnight in a humidified chamber as follows: Anti-C-NAP1 (Proteintech Europe, 66814-1); diluted 1:100; Anti-CEP164 diluted 1:1250 (AB clonal, A9964); Anti-γ-Tubulin diluted 1:100 (AB clonal A9657); Acetyl-TUBA1A diluted 1:100 (CliniSciences CSB-PA000127). Slides were washed three times in washing buffer (Phosphate-buffered saline with 0.1 % Tween® 20 Detergent) and incubated with secondary antibody for 1 h and Hoechst, 33342 Staining Dye Solution; diluted 1:5000 for 15 min (ab228551, abcam) at room temperature. Secondary antibodies were: Goat Anti-Mouse IgG H&L (Alexa Fluor® 647, red) (abcam, ab150115) and Goat Anti-Rabbit IgG H&L (Alexa Fluor® 488, green) (ab150077) diluted 1:500 or 1:1300, respectively. Slides were washed three times in washing buffer, mounted using Anti-Fade Fluorescence Mounting Medium - Aqueous, Fluoroshield (ab104135, abcam) and stored at −20 °C for future analysis. Unstained control samples were run to check and exclude autofluorescence. Specimens were imaged by fluorescent microscope (Nikon Eclipse) and confocal microscope LSM880 (Zeiss) controlled by the Zen blue software at high-magnifications fields (40x, 63x or 100x). High resolution images were analyzed with the Motic Image Plus 3.0 software, Nikon. For each image, we integrated intensity of pixels and percentage coverage of the color within/across cellular compartments by adjusting the pixel count for each nucleus. Manual pixel counts were also performed to determine the concentration of dye present in relation to the nuclei. Statistical analysis using r^2 was performed. From the data generated, it was observed a good correlation of dye positivity between manual assessment and the IF Motic Image Algorithm. At least one hundred nuclei were analyzed in three different area per tissue section.

2.7. Statistical analysis

Differences in overall survival and disease-free survival were measured by Kaplan-Meier curves using the log-rank test, at 95 % confidence intervals (CI). The Spearman rank test was used to assess the correlation between different centrosome-related markers expressed in PDACs tissues. Boxplots were used to visualize and compare centrosome-labelling at the single-cell level intensity related to nucleus in normal pancreas and PDAC tissues. Student t-test (2-tailed) or Wilcoxon-Mann-Whitney tests with

median differences at 95 % confidence interval (CI). Data are presented with mean, medians and ranges. For in-house cohort, the statistical analyses were carried out using Prism version 4.02 (GraphPad Software, Inc), GeneSpring R/bioconductor v.12.5 or R based package. Gene expression profiling analyses were performed using the R programming environment. All P values represent two-sided tests of statistical significance with p value < 0.05.

3. Results

3.1. Centrosome genes are dysregulated in the squamous PDAC subtype

To evaluate centrosomal related genes (CRGs) expression through different PDAC subtypes, we interrogated the expression data from the database (GSE36924), in which four distinct molecular subtypes named; Squamous, Pancreatic Progenitor, Immunogenic and Aberrantly Differentiated Endocrine Exocrine (ADEX) were identified [9]. Of the 564 CRGs, 482 (85,46 %) were available in the dataset. Unsupervised clustering analysis revealed the presence of three discrete groups (Fig. 1A). Interestingly, group 3 was mainly enriched for the squamous subtype and showed a high number of dysregulated CRGs compared to other subtypes ($p = 1.517727e-13$; Fig. 1B). Similarly, lymph-nodal dissemination and metastatic disease (N+ and stage IV status) were higher in group 3 than in groups 1 and 2. In the group 3, we identified a consistent number of over and under-expressed genes (Fig. 1A and B). Centriolar satellites and cilia/microtubule assembly were the top enriched terms of under-expressed genes. Conversely, over-expressed genes were significantly enriched for terms related to spindle assembly, chromosome segregation and centrosome duplication (Fig. 1C). This analysis identified a discrete group of sample that differ in their expression mostly in the squamous subtype known to correlate with poor survival.

3.2. A subset of CRGs is relevant for PDAC patients' prognosis

To determine if this classification has prognostic value, we used univariate Cox regression analysis. Out of 482 CRGs, 27 were associated with survival. Among them, 16 "positively" correlated with bad prognosis (beta >0) and 11 "negatively" with a good prognosis (beta <0) (Table S2). Unsupervised hierarchical clustering analysis indeed revealed that the 27 survival-related genes differ markedly in their expression values, clusters 5 and 2 respectively (Fig. 2A). For example, *PLK4* whose dysregulation drives centrosome amplification was identified in poor outcome group, supporting the reliability of the prognostic model [29,30] (Fig. 1A). To understand if the identified gene set has prognostic significance independent of tumour grade, we utilized an additional independent set of 80 PDAC cases named "CPTAC" [26]. Out of 479 CRGs, 93 genes positively or negatively correlated with survival (Table S2). Gene expression patterns for the 93 CRGs classified tumors into two discrete prognostic groups also for CPTAC database (Fig. 2B). Given that the two datasets revealed significant differences in the number of survival-related genes, in order to remove gross systematic differences the results were combined. A set of 14 common prognostic genes was identified, 5 negatively and 9 positively correlated with survival, respectively (Fig. 2C). For example, TRIM2 and TMEM63A involved in the ubiquitin pathway and centriolar vescicle transport were negatively correlated with survival [23]. In addition, PLK4,

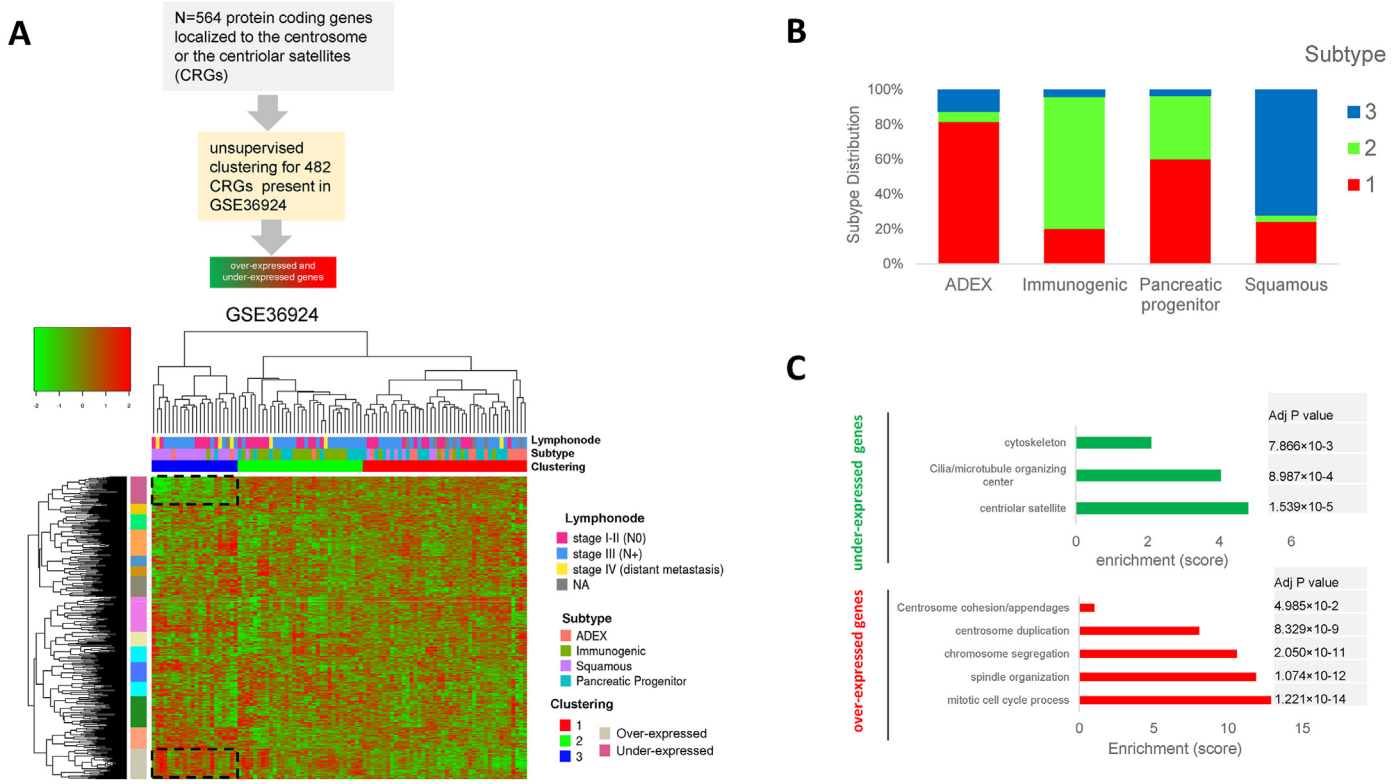

Fig. 1. Dysregulated CRGs characterize the squamous subtype. A) Unsupervised clustering of the CRGs related to the dataset GSE36924 highlights a cluster of samples enriched by the squamous subtype (columns) and two clusters of genes that appear differentially expressed. The annotation related to the Lymphatic invasion, Subtype and clustering have been added. The schematic workflow is represented at the top of the panel. **B)** the barplots in the panel represent the molecular subtype distribution across the three clusters identified. **C)** Gene ontology (GO) terms for the over-representation analysis of the under-expressed (green) and over-expressed (red) genes.

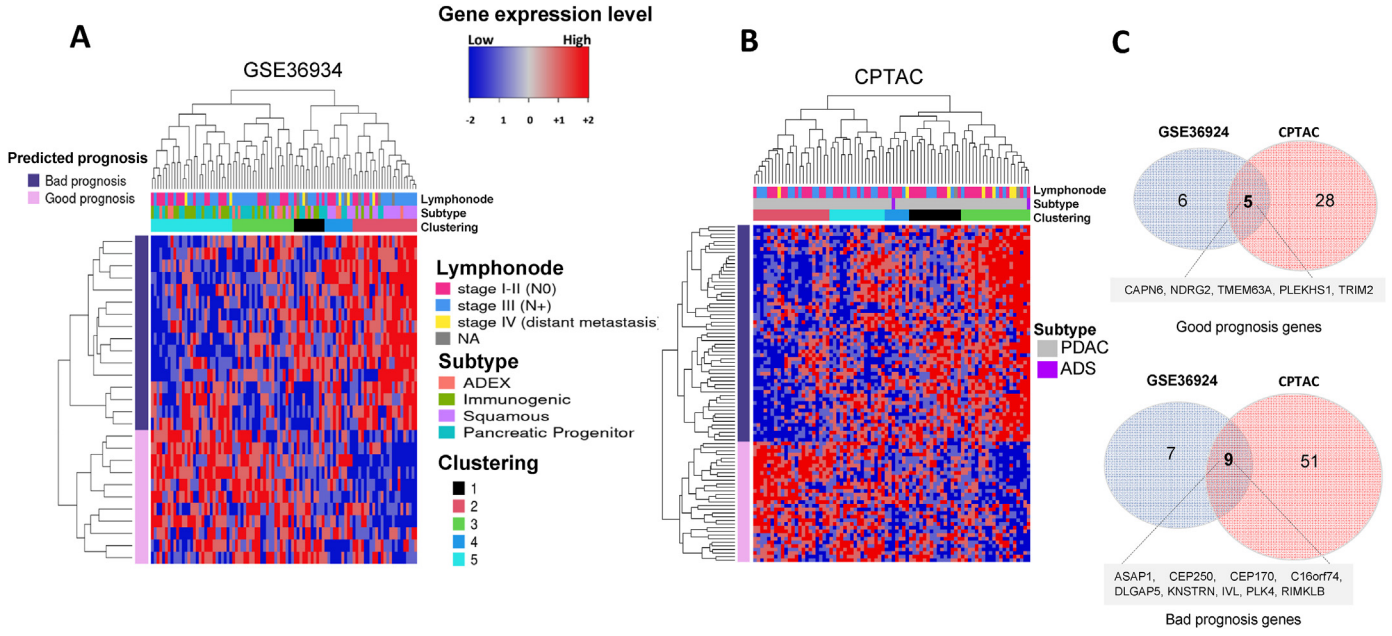

Fig. 2. A subset of CRGs predicts prognosis of PDAC patients: A) Unsupervised clustering related to the expression of the bad and good prognosis CRGs uncovered from the Cox univariate analysis for the training and test dataset **B)**, respectively. The annotations related to the prognostic group, Lymphatic invasion, Subtype and clustering have been added. **C)** Venn plots show the common Bad and Good CRGs identified between the two cohorts.

CEP250, CEP170 and ASAP1 involved in centrosome duplication, centrosome cohesion and microtubule organization activities positively correlated with survival (Table S3) [20,21,23,28]. The results revealed previously unknown CRGs with prognostic relevance in PDAC.

3.3. Appendages and centrosome cohesion components are related to PDAC prognosis

We next compared the common good and poor prognostic genes with the Kaplan-Meier method. We found that PDAC patients expressing bad prognosis genes exhibited about 5-fold increased risk of death compared to good prognostic group, HR = 0.18 (0.08–0.39 95 % CI) *p=0.0001* (Fig. 3A). Similar results were observed also for the CPTAC dataset, HR = 0.20 (0.08–0.50 95 % CI) *p=0.00016* (Fig. 3B). *CEP250* and *CEP170* were expressed at high levels in PDAC tissues and correlated with prognosis of PDAC patients in both the databases (Fig. 3C and D and Table S3). Multivariate analysis for CEP250 in both CPTAC and GSE36924 datasets confirmed a significant effect on patients' outcomes (Fig. S1B). To further clarify the effective impact of candidate prognostic genes, we explored their expression profiles in the TCGA database using as reference normal pancreatic tissues. A number of bad prognosis genes (7 out of 9; 77,7 %) including CEP250 and CEP170 exhibited higher expression in PDAC than in normal pancreas tissues (Fig. 4A and B). In contrast, no differential expression was found for 3 out of the 5 good prognosis genes. Unexpectedly, two genes "TRIM2 and CAPN6" that negatively correlated with survival were significantly higher in PDACs than in normal tissues (Fig. 4A). As we did not identify effective protective prognostic genes, we explored additional centrosome protein-encoding genes candidates localized to the centriolar DAPs, which are crucial in the process of primary cilia formation [16]. Notably, the systematic exploration of HPA database revealed CEP164 expression as a pancreas-specific marker reduced in PDACs related to normal pancreas tissues (Figs. S2A and B). In addition, survival analysis disclosed that PDAC patients with low expression levels of *CEP164* exhibited shorter survival than those with high expression (Fig. S2C). Therefore, reduced expression of CEP164 represented a candidate gene for further exploration.

3.4. The centrosome cohesion factor CEP250 is overexpressed in PDAC with supernumerary centrosomes

In addition to the sDAPs, CEP170 is also localized to the centriole proximal end in a CEP250-dependent manner [16,20]. Thus, *in-silico* predictions suggested a predominant dysregulation of the centrosome cohesion system.

We collected a series of 23 human FFPE PDAC with follow-up information to verify CEP250 expression by immunohistochemistry (IHC). Normal pancreatic tissues were used for comparison. In normal pancreas, CEP250 exhibited weak staining and marked mainly exocrine glandular cells. In contrast, the large majority of PDACs displayed a moderate (7/23; 30 %) or high (10/23; 44 %) positivity. Fewer cancer tissues (6/23; 26 %) were weakly stained (Fig. 4C). To accurately quantify CEP250 expression in normal pancreas and PDAC FFPE tissues, we used immunofluorescence. Serial sections from the same tissues were also labelled for the PCM protein γ-tubulin, as reference to mark centrosome number per cell. In all samples, CEP250 showed quantifiable results. Normal pancreatic glands contained often single or two centrosome-marked CEP250 foci (~12/100 cells). In contrast PDACs generally displayed voluminous and greater CEP250-labelled centrosomes than the normal pancreas (Fig. 5A). Having confirmed CEP250 overexpression in PDAC, we explored γ-tubulin staining. In normal pancreas, anti−γ-tubulin resulted in one focus with an irregularly shaped pattern. Interestingly, PDACs contained supernumerary centrosomes marked by more than two distinct γ-tubulin foci. Statistical analysis revealed a positive correlation between CEP250 and centrosome amplification (CA) in a subset of PDAC samples (Fig. 5A and Fig. S2D). Taken together, these findings suggested that CEP250-overexpressing PDACs exhibited a greater extent of centrosomes abnormalities than CEP250-low expressing groups, confirming that its dysregulation participates in PDAC pathogenesis.

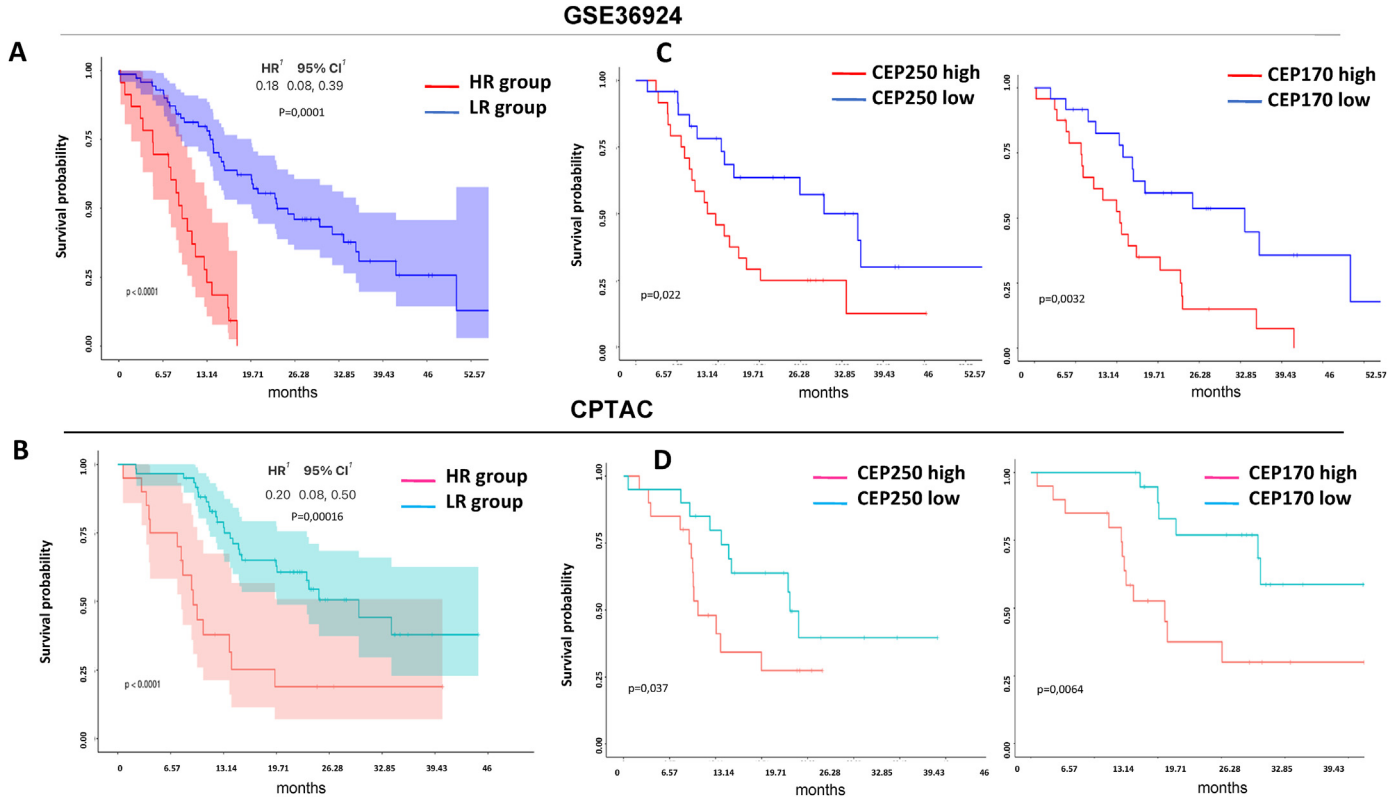

Fig. 3. Linker and centriolar appendage genes are associated with prognosis of PDAC patients. A) and **B)** Kaplan-Meier curves comparing the High-Risk (HR) and the Low-Risk (LR) group in GSE36924 and the CPTAC cohort, respectively. **C)** and **D)** Kaplan-Meier curves comparing the patients having altered expression of the two bad prognosis genes CEP250 and CEP170: higher than the 3rd quartile (high) vs lower of the 1st quartile (low).

3.5. Centrosome cohesion is relevant for the clustering of amplified centrosomes

To explore the effects of CEP250 over-expression on centriole amplification, we used multiplexed immunofluorescence to visualize centrosome amplification by γ-tubulin (green) in relation to CEP250 (red) in normal and PDAC tissues. High-resolution microscopy was used to acquire whole cell volumes in which to scan for centrosomes.

We found that CEP250 and γ-tubulin colocalized at the centrosome as discrete foci in normal pancreatic tissues (Fig. S3A). In the PDAC tissue sample, we detected centrosome amplification as evidenced by the presence of > 2γ-tubulin foci per cell. Strikingly, a significant number of cells exhibited large clustered γ-tubulin-labelled centrosomes that appeared linked together by CEP250 ring and planar-shaped structures (Fig. 5B and Fig. S3A). Interestingly, the diameter of the CEP250 ring structures appeared to increase with the number of γ-tubulin foci (Fig. 5B). These findings provided evidence that amplifed centrosomes are connected to each other through aberrant centrosome linker structures in PDACs.

3.6. Overexpression of CEP250 is associated to reduced CEP164 and loss of primary cilia in PDACs

Having confirmed an association between CEP250 and centrosome anomalies, we were interested in understanding if the expression of the distal appendage protein CEP164 is related to CEP250 in normal pancreas and PDACs tissues. We found a strong cytoplasmic/membranous expression of CEP164 in normal pancreatic tissues by IHC. In contrast, weak to moderate cytoplasmic/membranous immunoreactivity was observed in most PDACs, confirming bioinformatics predictions (Fig. 5C). Correlative immunofluorescence-light microscopy indeed revealed that CEP164-labelled centrosomes tended to be reduced in PDACs as compared to normal pancreas (Figs. S3B and C). As CEP164 is connected to ciliogenesis, immunofluorescence was performed to visualize in the same tissues acetylated tubulin, a marker for primary cilia. Importantly, in normal pancreatic glands, we detected that most cells displayed prominent primary cilia, which tend to be markedly reduced in PDACs (Fig. 5C and Fig. S3C). Reduced CEP164 and cilia staining appeared to be correlated in a subset of PDAC samples (Fig. S3C). We next used multiplexed immunofluorescence to visualize CEP164 (green) and CEP250 (red) at centrosomes of normal and PDAC tissues. Centrosomes that were labelled with both anti-CEP250 and CEP164 antibodies were often detected in normal pancreatic cells (Fig. 5D). We observed a significant deviation from this pattern in PDAC tissues overexpressing CEP250. Intriguingly, CEP250-labelled centrosomes not marked by CEP164, tended to be more separated “10 μm apart” placing them on opposite sides of the cell or nucleus (Fig. 5D). Conversely, CEP164-high expressing PDACs appeared as large “ring-like” structures sporadically marked by a single CEP250 spot (Fig. S3B). Indeed, CEP250-high expressing PDAC exhibited a higher centrosome separation than those with moderate expression or normal pancreas (Fig. 5E). Consistently, quantification of centrosomes marked by CEP250 and CEP164 revealed an inverse correlation in a subset of PDACs (Fig. 5E). In summary, our findings suggested that CEP250-overexpressing PDACs exhibit defects in centrosome cohesion also related to dysregulation of distal appendages.

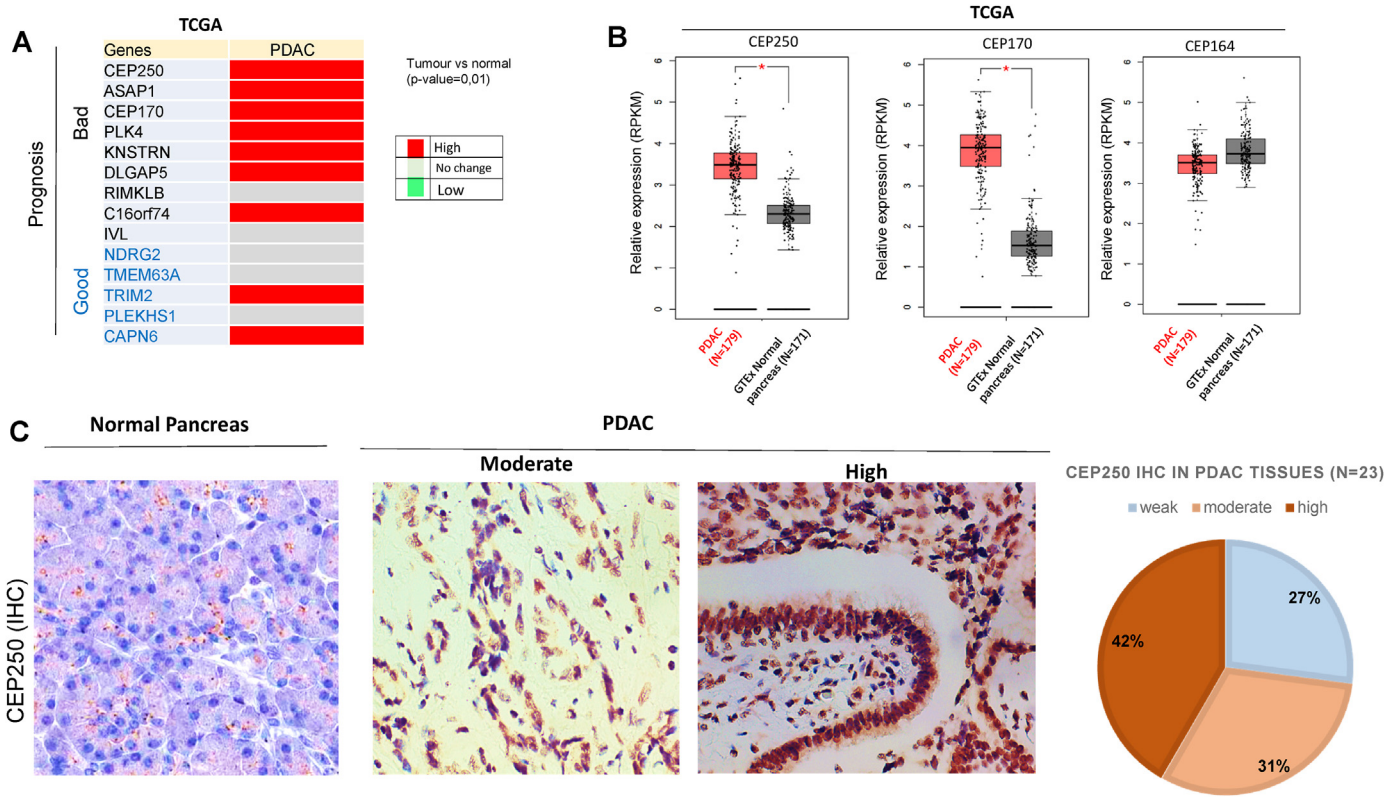

Fig. 4. CEP250 is overexpressed in PDAC A) Gene expression profiles of candidate good (blue) and bad (black) prognostic genes in PDAC and related normal pancreas from TCGA and GTEx databases. High (red) and low (green) expression ($p < 0,05$) in PDAC are indicated. No significant changes ($p > 0,05$) are in grey. **B)** Gene expression profiles of CEP250, CEP170 and CEP164 in PDAC (n = 179) vs GTEx (n = 171) are shown by Box-plots. *$P < 0,05$. **C)** Left, representative pictures show immunohistochemical (IHC) staining results of CEP250 in normal pancreas and PDAC tissues. Magnification (40×). On the right, the CEP250 IHC results are summarized by the pie chart. PDACs (n = 23).

3.7. *CEP250 expression in PDAC impacts on patients' prognosis*

The association of centrosome cohesion abnormalities with poor prognostic indicators in pancreatic cancer is unknown. Therefore, we examined CEP250 expression in 23 PDACs and sought associations with clinicopathologic parameters including age, sex, tumor size, grade/extent of differentiation, stage, lymph node metastasis, survival parameters and clinical response to treatment. For statistical purpose, PDACs displaying weak or moderate CEP250 IHC staining were defined low and compared to the CEP250-high expressing group. We found that CEP250 expression mostly influenced the relapse (Table S1). Next we then analyzed CEP250 in relation with overall (OS) and disease free survival (DFS). Indeed, CEP250-high PDACs exhibited shorter OS and DFS than the CEP250-low group. The median DFS was 8,4 months in the CEP250-high group and 15,9 months in the CEP250-low group, respectively *p=0.030*. Consistently, the median OS was 14.9 months in the CEP-250-high group and 25.3 months in the CEP-250 low group; p = 0.030 (Fig. 6A and B). Because CEP250-High PDAC patients were related to "relapse", we investigated whether CEP250 expression correlated with responses to nab paclitaxel plus gemcitabine chemotherapy-based treatment. Seventeen "relapsed" patients treated with such a therapeutic regimen were available. Of note, 81 % of the CEP250-high patients did not respond to therapy. In stark contrast, 82 % of the CEP250-low patients exhibited good clinical responses (Fig. 6C). Consistently, median PFS for the first-line therapy was shorter in CEP250-high than in CEP250-low expressing PDACs, 3,4 versus 6 months respectively; p = 0.039 (Fig. S3D). The results confirmed CEP250 expression as probable predictor of clinical outcomes in PDAC patients.

4. Discussion

Despite the efforts in understanding the aggressive nature of PDAC, these have not translated into a breakthrough in clinical care, for the majority of patients. So it is crucial to identify novel targets for its treatment. High-throughput genomic studies provided evidences that the aggressive behaviour of PDAC may be due to the remarkably complex mutational landscape, extensive intratumor heterogeneity and chromosomal instability. Centrosome amplification (CA) is a well-known mediator of chromosomal instability. However, whether centrosome-related genes influence PDAC prognosis has not been tested [29,30].

We here found a set of centrosome genes with prognostic relevance in PDAC patients. Among them *PLK4,* a well-known master regulator of centriole duplication that served as positive control for the assessment of other prognostic genes [29,30]. *In vitro* studies on the role of PLK4 in centriole biogenesis have mostly been conducted by its over-expression, resulting in the formation of abnormal ring-shaped clusters of procentrioles on the maternal centriole named centriole rosettes [31].

Interestingly, *CEP250* and *CEP170*, involved in centrosome linker and sDAPs structures were also over-expressed and related to the prognosis. Recently, a CA-signature based on the expression of 20 centrosome genes (CA20) has been developed, demonstrating that high CA20 is associated with poor patient's survival in several cancer types [32]. Some of genes identified here, mostly *CEP250* and *CEP170* were not included in CA20 panel, suggesting that centrosome genes with prognostic relevance may be cancer-specific. Therefore, panels for CA should be modeled prioritizing candidate genes with biological relevance or by tissue-specific direct

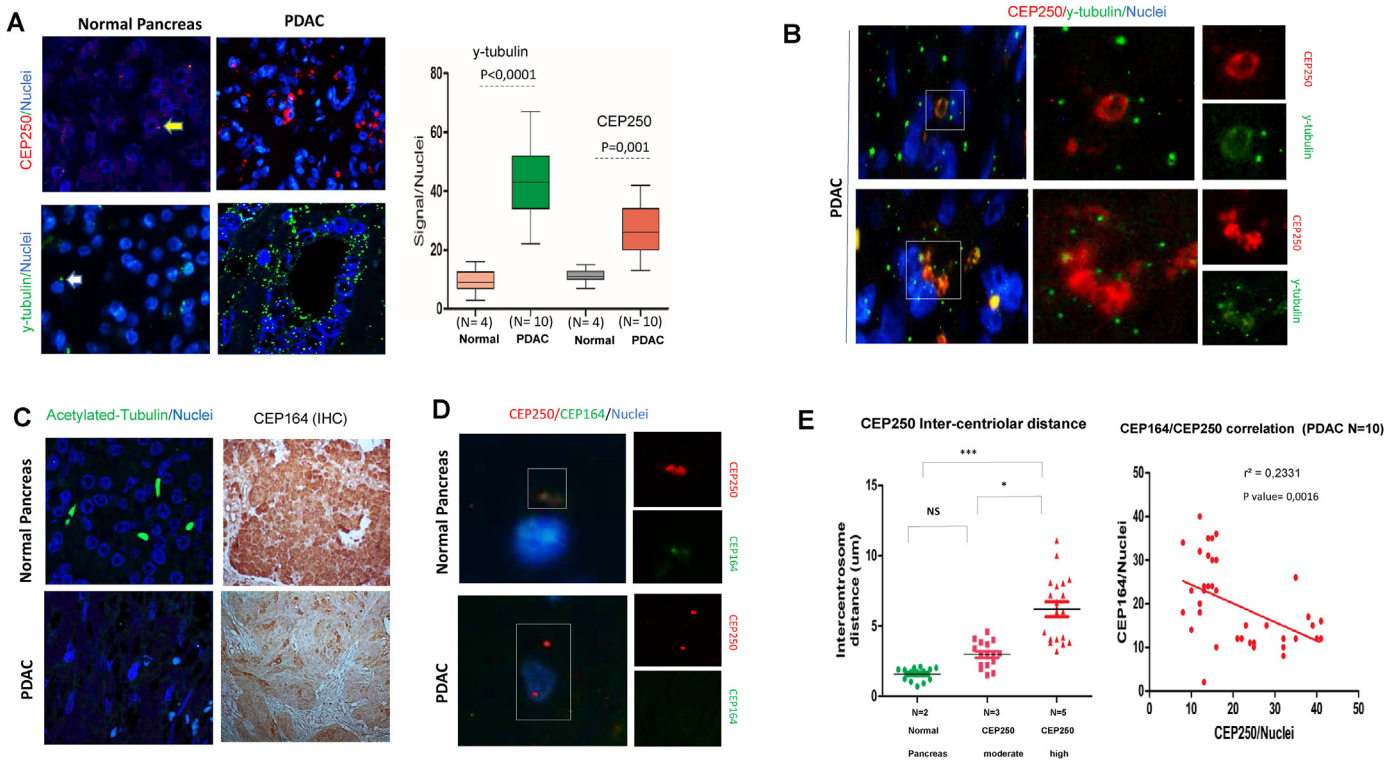

Fig. 5. Centrosome-cohesion is relevant for the clustering of amplified centrosomes**. A)** Left, normal pancreas and PDAC tissues stained with CEP250 (red), γ-tubulin (green). Nuclei in blue. Magnifications (40×). Right, quantification of γ-tubulin and CEP250-labelled centrosomes in normal pancreas (n = 4) vs PDACs (n = 10) is shown by box-plot. The *P values* were evaluated using unpaired t tests. **B)** PDAC tissues stained with CEP250 (red), γ-tubulin (green). Nuclei in blue. The right panels show high-resolution images of amplified centrioles (green) linked together by circular and planar-shaped CEP250 arrangements (red). Bar 10 μm. **C)** Left, normal pancreas and PDAC tissue stained with acetylated-tubulin (green). Nuclei in blue. Right, CEP164 staining in normal pancreas and PDAC by immunohistochemistry (IHC). **D)** Normal pancreas and PDAC tissues stained with CEP250 (red), CEP164 (green). Nuclei in blue. The right panels show high-resolution images, Bar 10 μm. In normal pancreatic cells, the partial colocalization of CEP250 and CEP164 results in closely linked centrosomes. In PDAC, loss of CEP164 results in distanced CEP250-labelled centrosomes **D)** Left, centrosome separation (um) is quantified in normal pancreas, CEP250-moderate or CEP250-high PDACs by the box.plot. Right, the negative association between CEP164 and CEP250-labbeled centrosomes in PDACs is shown by scatterplot. NS, not significant; *p < 0,05; ***p < 0.001.

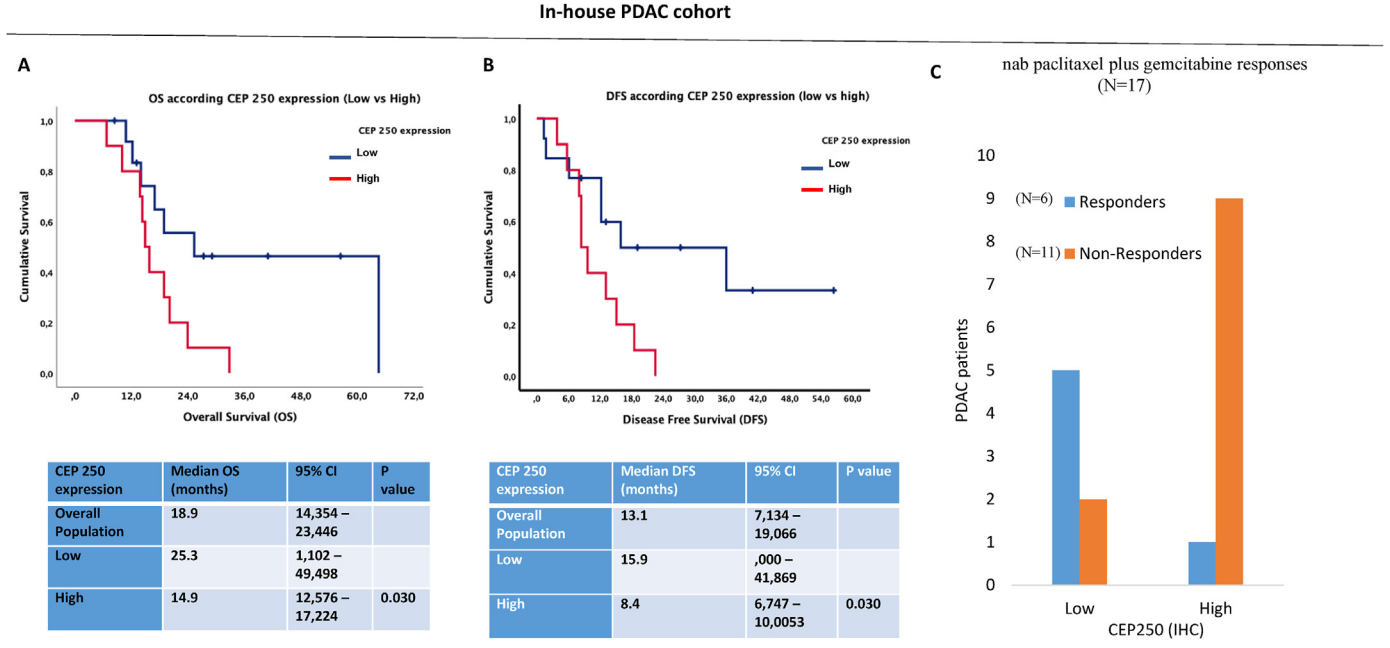

CEP 250 expression	Median OS (months)	95% CI	P value
Overall Population	18.9	14,354 – 23,446	
Low	25.3	1,102 – 49,498	
High	14.9	12,576 – 17,224	0.030

CEP 250 expression	Median DFS (months)	95% CI	P value
Overall Population	13.1	7,134 – 19,066	
Low	15.9	,000 – 41,869	
High	8.4	6,747 – 10,0053	0.030

Fig. 6. CEP250 expression predicts PDAC prognosis. A) CEP250 expression in relation to overall survival of patients with PDACs is shown by Kaplan-Meier curve. Down, the table shows the median survival "in months" for the entire cohort and for each sub-group. **B)** CEP250 is related to disease-free survival (DFS) of patients with PDACs. Down, the median DFS "in months" is reported in table. **C)** The graph shows the expression of CEP250 in patients who were treated with nab paclitaxel plus gemcitabine first-line therapy. The patients are classified as Responders (N = 6) and non-Responders (N = 11).

experimental validation. We also identified *CEP164* as a relevant pancreas enriched protein downregulated in PDAC. Therefore, together with increased expression of CEP170, mainly localized at sDAPs, it seems likely that in PDAC the remodelling of "mother centriole and its appendages" composition is at least responsible for cancer progression. CEP170 is also located at the proximal ends of centriole through the centrosome linker factor CEP250 [19,20]. Our experimental findings indeed suggested that about half of PDACs exhibited a consistent overexpression of CEP250 compared to normal pancreas. Notably, PDACs tissues with extra centrosomes were linked together by aberrant circular and planar-shaped CEP250 arrangements. In this condition, CEP250 could play a role in pseudo-bipolar spindle formation in cells with supernumerary centrosomes, which occasionally can give rise to aneuploid and transformed daughter cells. However, how and why CEP250 that only associates at the proximal end of centrioles contributes to γ-tubulin clustering is presently unclear. Notably, CEP250-overexpressing PDACs displayed a prominent centrosome separation characterized by CEP164 removal at centrosomes. Our findings are in line with recent *in vitro* observations that NEK2 kinase, a well-known CEP250 regulator, not only promotes centriole separation but also CEP164 removal from the centrosomes [33]. Why centriolar appendages, centrosome duplication and cohesion are closely interdependent is matter of debated. We indeed found that reduced CEP164 and defects in primary cilia in PDAC could be interdependent. It remains to establish whether CEP164 downregulation might be one underlying mechanism that contributes to the loss of cilia in PDAC cellular models *in vitro*.

We confirmed that the overall survival and disease free survival of patients as well as the probability of metastatic distant relapse is influenced by CEP250 expression. Interestingly, almost none of the 11 "relapsed" CEP250-high expressing PDAC patients who received gemcitabine plus nab-paclitaxel therapy achieved a clinical response. In contrast, a few PDACs displaying weak CEP250 expression were long-term survivors or responsive to therapeutic treatment. However, given the small sample size of our validation cohort, the prognostic potential of centrosome-related genes the needs to be further assessed in larger cohorts of unselected patients with PDAC.

Notably, a recent study showed that patients low levels of CEP170 had a better prognosis and a mutational signature associated with defective DNA repair [34,35]. In this scenario, low levels of CEP170 and CEP250 could render tumoral cells defective in homologous recombination (HR) pathways hypersensitive to anticancer treatments, thus increasing patient survival. It is interesting to note that several components of the DNA damage response (DDR) have been identified at the centrosome as the checkpoint proteins ATM, ATR, BRCA1, BRCA2, or PARPs play an important role in PDAC [34]. Thus, considering collectively that induction of DNA double strand breaks (DSBs) is a first-line therapeutic approach, further understanding of the centrosome role in DNA repair will open new research lines and therapeutic avenues in PDAC oncology.

5. Conclusions

In summary, alterations in centrosome cohesion and centriolar appendages have effect on the survival of patients with PDAC and could be exploited as potential targets for future investigations.

Authors' contributions

GG, MCC, FPC, LC, FN and MP designed, developed and interpreted bioinformatics analysis. LC, EDS, GG and NF, PP, and ML provided FFPE normal pancreas and PDAC samples. AM, GC, NF and MP performed and interpreted IHC results. AM, GC, GP conducted and interpreted multiplexed immunofluorescence results on tissues samples supervised by MP. GG and MP performed statistical analyses on clinical PDAC and interpreted results. GG, MP and LC drafted and critically revised the manuscript. GG and MP supervised the study. GG conceived the study. All authors have read and approved the final manuscript.

Funding

This study was supported by a grant from the Italian Ministry of University and Research (MIUR FFABR grant n.4982) to M.P.

Ethics approval and consent to participate

The study protocol was approved by the Institutional Review Board (IRB) of the Policlinico Ospedali Riuniti, University of Foggia (Comitato Etico Area 1, 128/CE/2023).

Consent for publication

Not applicable.

Competing interests

The authors have declared no competing interest.

Availability of data and materials

The datasets used and/or analyzed during the current study are available from the corresponding author on reasonable request.

Acknowledgements

We would like to thank lab technicians from different hospital institutions for the preparation of samples used for in situ analyses. We are thankful to Roman Polishchuk and Brunella Franco team, Tigem Institute, Naples, for the use of the services, facilities and technical assistance on high resolution imaging.

Abbreviations

PDAC	Pancreatic ductal adenocarcinoma
CRGs	Centrosome-related genes
DAPs	Distal appendages
sDAPs	subdistal appendages
DDR	DNA damage response
HPA	Human Protein Atlas
TCGA	Cancer Genome Atlas
GTEx	Genotype-Tissue Expression atlas
IHC	Immunohistochemistry
CPH	Cox proportional hazard.

Appendix A. Supplementary data

Supplementary data to this article can be found online at https://doi.org/10.1016/j.pan.2024.06.010.

References

[1] Stoffel EM, Brand RE, Goggins M. Pancreatic cancer: changing epidemiology and new approaches to risk assessment, early detection, and prevention. Gastroenterology 2023 Apr;164(5):752–65. https://doi.org/10.1053/j.gastro.2023.02.012. Epub 2023 Feb 18. PMID: 36804602; PMCID: PMC10243302.

[2] Halbrook CJ, Lyssiotis CA, Pasca di Magliano M, Maitra A. Pancreatic cancer: advances and challenges. Cell 2023 Apr 13;186(8):1729–54. https://doi.org/

10.1016/j.cell.2023.02.014. PMID: 37059070; PMCID: PMC10182830.
[3] Von Hoff DD, Ervin T, Arena FP, Chiorean EG, Infante J, Moore M, Seay T, Tjulandin SA, Ma WW, Saleh MN, et al. Increased survival in pancreatic cancer with nab-paclitaxel plus gemcitabine. N Engl J Med 2013;369:1691–703. https://doi.org/10.1056/NEJMoa1304369.
[4] Burris HA 3rd, Moore MJ, Andersen J, Green MR, Rothenberg ML, Modiano MR, Cripps MC, Portenoy RK, Storniolo AM, Tarassoff P, Nelson R, Dorr FA, Stephens CD, Von Hoff DD. Improvements in survival and clinical benefit with gemcitabine as first-line therapy for patients with advanced pancreas cancer: a randomized trial. J Clin Oncol 1997 Jun;15(6):2403–13. https://doi.org/10.1200/JCO.1997.15.6.2403. Corrected and republished in: J Clin Oncol. 2023 Dec 20;41(36):5482-2413. PMID: 9196156.
[5] Conroy T, Desseigne F, Ychou M, Bouché O, Guimbaud R, Bécouarn Y, Adenis A, Raoul JL, Gourgou-Bourgade S, de la Fouchardière C, Bennouna J, Bachet JB, Khemissa-Akouz F, Péré-Vergé D, Delbaldo C, Assenat E, Chauffert B, Michel P, Montoto-Grillot C, Ducreux M. Groupe tumeurs digestives of unicancer; PRODIGE intergroup. FOLFIRINOX versus gemcitabine for metastatic pancreatic cancer. N Engl J Med 2011 May 12;364(19):1817–25. https://doi.org/10.1056/NEJMoa1011923. PMID: 21561347.
[6] Maitra A, Adsay NV, Argani P, Iacobuzio-Donahue C, De Marzo A, Cameron JL, Yeo CJ, Hruban RH. Multicomponent analysis of the pancreatic adenocarcinoma progression model using a pancreatic intraepithelial neoplasia tissue microarray. Mod Pathol 2003;16:902–12. https://doi.org/10.1097/01.MP.0000086072.56290.FB.
[7] Makohon-Moore AP, Matsukuma K, Zhang M, Reiter JG, Gerold JM, Jiao Y, Sikkema L, Attiyeh MA, Yachida S, Sandone C, et al. Precancerous neoplastic cells can move through the pancreatic ductal system. Nature 2018;561:201–5. https://doi.org/10.1038/s41586-018-0481-8.
[8] Hingorani SR, Wang L, Multani AS, Combs C, Deramaudt TB, Hruban RH, Rustgi AK, Chang S, Tuveson DA. Trp53R172H and KrasG12D cooperate to promote chromosomal instability and widely metastatic pancreatic ductal adenocarcinoma in mice. Cancer Cell 2005;7:469–83. https://doi.org/10.1016/j.ccr.2005.04.023.
[9] Collisson EA, Sadanandam A, Olson P, Gibb WJ, Truitt M, Gu S, Cooc J, Weinkle J, Kim GE, Jakkula L, et al. Subtypes of pancreatic ductal adenocarcinoma and their differing responses to therapy. Nat Med 2011;17:500–3. https://doi.org/10.1038/nm.2344.
[10] Moffitt RA, Marayati R, Flate EL, Volmar KE, Loeza SG, Hoadley KA, Rashid NU, Williams LA, Eaton SC, Chung AH, et al. Virtual microdissection identifies distinct tumor- and stroma-specific subtypes of pancreatic ductal adenocarcinoma. Nat Genet 2015;47:1168–78. https://doi.org/10.1038/ng.3398.
[11] Bailey P, Chang DK, Nones K, Johns AL, Patch AM, Gingras MC, Miller DK, Christ AN, Bruxner TJ, Quinn MC, et al. Genomic analyses identify molecular subtypes of pancreatic cancer. Nature 2016;531:47–52. https://doi.org/10.1038/nature16965.
[12] Schatten H. Centrosome dysfunctions in cancer. Adv Anat Embryol Cell Biol 2022;235:43–50. https://doi.org/10.1007/978-3-031-20848-5_4. PMID: 36525110.
[13] Bornens M. The centrosome in cells and organisms. Science 2012 Jan 27;335(6067):422–6. https://doi.org/10.1126/science.1209037. PMID: 22282802.
[14] Vasquez-Limeta A, Loncarek J. Human centrosome organization and function in interphase and mitosis. Semin Cell Dev Biol 2021 Sep;117:30–41. https://doi.org/10.1016/j.semcdb.2021.03.020. Epub 2021 Apr 6. PMID: 33836946; PMCID: PMC8465925.
[15] Dang H, Schiebel E. Emerging roles of centrosome cohesion. Open Biol 2022 Oct;12(10):220229. https://doi.org/10.1098/rsob.220229. Epub 2022 Oct 26. PMID: 36285440; PMCID: PMC9597181.
[16] Ma D, Wang F, Teng J, Huang N, Chen J. Structure and function of distal and subdistal appendages of the mother centriole. J Cell Sci 2023 Feb 1;136(3):jcs260560. https://doi.org/10.1242/jcs.260560. Epub 2023 Feb 2. PMID: 36727648.
[17] Kumar D, Reiter J. How the centriole builds its cilium: of mothers, daughters, and the acquisition of appendages. Curr Opin Struct Biol 2021 Feb;66:41–8. https://doi.org/10.1016/j.sbi.2020.09.006. Epub 2020 Nov 4. PMID: 33160100.
[18] Čajánek L, Nigg EA. Cep164 triggers ciliogenesis by recruiting Tau tubulin kinase 2 to the mother centriole. Proc Natl Acad Sci U S A 2014 Jul 15;111(28):E2841–50. https://doi.org/10.1073/pnas.1401777111. Epub 2014 Jun 30. PMID: 24982133; PMCID: PMC4104846.
[19] Theile L, Li X, Dang H, Mersch D, Anders S, Schiebel E. Centrosome linker diversity and its function in centrosome clustering and mitotic spindle formation. EMBO J 2023 Sep 4;42(17):e109738. https://doi.org/10.15252/embj.2021109738. Epub 2023 Jul 4. PMID: 37401899; PMCID: PMC10476278.
[20] Zhang X, Chen MH, Wu X, Kodani A, Fan J, Doan R, Ozawa M, Ma J, Yoshida N, Reiter JF, Black DL, Kharchenko PV, Sharp PA, Walsh CA. Cell-type-specific alternative splicing governs cell fate in the developing cerebral cortex. Cell 2016 Aug 25;166(5):1147–1162.e15. https://doi.org/10.1016/j.cell.2016.07.025. PMID: 27565344; PMCID: PMC5248659.
[21] Remo A, Li X, Schiebel E, Pancione M. The centrosome linker and its role in cancer and genetic disorders. Trends Mol Med 2020 Apr;26(4):380–93. https://doi.org/10.1016/j.molmed.2020.01.011. Epub 2020 Feb 18. PMID: 32277932.
[22] Mazo G, Soplop N, Wang WJ, Uryu K, Tsou MF. Spatial control of primary ciliogenesis by subdistal appendages alters sensation-associated properties of cilia. Dev Cell 2016 Nov 21;39(4):424–37. https://doi.org/10.1016/j.devcel.2016.10.006. Epub 2016 Nov 3. PMID: 27818179; PMCID: PMC5125554.
[23] Thul PJ, Lindskog C. The human protein atlas: a spatial map of the human proteome. Protein Sci 2018;27:233–44.
[24] Lonsdale J, Thomas J, Salvatore M, et al. The genotype-tissue expression (GTEx) project. Nat Genet 2013;45:580–5. https://doi.org/10.1038/ng.2653.
[25] Tang Z, Li C, Kang B, Gao G, Li C, Zhang Z. GEPIA: a web server for cancer and normal gene expression profiling and interactive analyses. Nucleic Acids Res 2017 Jul 3;45(W1):W98–102. https://doi.org/10.1093/nar/gkx247. PMID: 28407145; PMCID: PMC5570223.
[26] Cao L, Huang C, Cui Zhou D, Hu Y, Lih TM, Savage SR, Krug K, Clark DJ, Schnaubelt M, Chen L, da Veiga Leprevost F, Eguez RV, Yang W, Pan J, Wen B, Dou Y, Jiang W, Liao Y, Shi Z, Terekhanova NV, Cao S, Lu RJ, Li Y, Liu R, Zhu H, Ronning P, Wu Y, Wyczalkowski MA, Easwaran H, Danilova L, Mer AS, Yoo S, Wang JM, Liu W, Haibe-Kains B, Thiagarajan M, Jewell SD, Hostetter G, Newton CJ, Li QK, Roehrl MH, Fenyö D, Wang P, Nesvizhskii AI, Mani DR, Omenn GS, Boja ES, Mesri M, Robles AI, Rodriguez H, Bathe OF, Chan DW, Hruban RH, Ding L, Zhang B, Zhang H, Clinical Proteomic Tumor Analysis Consortium. Proteogenomic characterization of pancreatic ductal adenocarcinoma. Cell 2021 Sep 16;184(19):5031–5052.e26. https://doi.org/10.1016/j.cell.2021.08.023. PMID: 34534465; PMCID: PMC8654574.
[27] Raudvere U, Kolberg L, Kuzmin I, Arak T, Adler P, Peterson H, Vilo J. g:Profiler: a web server for functional enrichment analysis and conversions of gene lists (2019 update). Nucleic Acids Res 2019 Jul 2;47(W1):W191–8. https://doi.org/10.1093/nar/gkz369. PMID: 31066453; PMCID: PMC6602461.
[28] Cerulo L, Pezzella N, Caruso FP, Parente P, Remo A, Giordano G, Forte N, Busselez J, Boschi F, Galiè M, Franco B, Pancione M. Single-cell proteo-genomic reveals a comprehensive map of centrosome-associated spliceosome components. iScience 2023 Apr 10;26(5):106602. https://doi.org/10.1016/j.isci.2023.106602. PMID: 37250316; PMCID: PMC10214398.
[29] Ansari D, Del Pino Bellido C, Bauden M, Andersson R. Centrosomal abnormalities in pancreatic cancer: molecular mechanisms and clinical implications. Anticancer Res 2018 Mar;38(3):1241–5. https://doi.org/10.21873/anticanres.12345. PMID: 29491046.
[30] Mittal K, Kaur J, Sharma S, Sharma N, Wei G, Choudhary I, Imhansi-Jacob P, Maganti N, Pawar S, Rida P, Toss MS, Aleskandarany M, Janssen EA, Søiland H, Gupta MV, Reid MD, Rakha EA, Aneja R. Hypoxia drives centrosome amplification in cancer cells via HIF1α-dependent induction of polo-like kinase 4. Mol Cancer Res 2022 Apr 1;20(4):596–606. https://doi.org/10.1158/1541-7786.MCR-20-0798. PMID: 34933912; PMCID: PMC8983505.
[31] Ozcan SC, Kalkan BM, Cicek E, et al. Prolonged overexpression of PLK4 leads to formation of centriole rosette clusters that are connected via canonical centrosome linker proteins. Sci Rep 2024;14:4370. https://doi.org/10.1038/s41598-024-53985-2.
[32] de Almeida BP, Vieira AF, Paredes J, Bettencourt-Dias M, Barbosa-Morais NL. Pan-cancer association of a centrosome amplification gene expression signature with genomic alterations and clinical outcome. PLoS Comput Biol 2019 Mar 11;15(3):e1006832. https://doi.org/10.1371/journal.pcbi.1006832. PMID: 30856170; PMCID: PMC6411098.
[33] Viol L, Hata S, Pastor-Peidro A, Neuner A, Murke F, Wuchter P, Ho AD, Giebel B, Pereira G. Nek2 kinase displaces distal appendages from the mother centriole prior to mitosis. J Cell Biol 2020 Mar 2;219(3):e201907136. https://doi.org/10.1083/jcb.201907136. PMID: 32211891; PMCID: PMC7055001.
[34] Rodríguez-Real G, Domínguez-Calvo A, Prados-Carvajal R, Bayona-Feliú A, Gomes-Pereira S, Balestra FR, Huertas P. Centriolar subdistal appendages promote double-strand break repair through homologous recombination. EMBO Rep 2023 Oct 9;24(10):e56724. https://doi.org/10.15252/embr.202256724. Epub 2023 Sep 4. PMID: 37664992; PMCID: PMC10561181.
[35] Johnson CA, Malicki JJ. The nuclear arsenal of cilia. Dev Cell 2019 Apr 22;49(2):161–70. https://doi.org/10.1016/j.devcel.2019.03.009. PMID: 31014478.